

Study of primordial non-Gaussianity f_{NL} and g_{NL} with the cross-correlations between the scalar-induced gravitational waves and the cosmic microwave background

Zhi-Chao Zhao¹, Sai Wang^{a,2}, Jun-Peng Li^{3,4},
Kazunori Kohri^{5,6,7}

¹Department of Applied Physics, College of Science, China Agricultural University, 17 Qinghua East Road, Haidian District, Beijing 100083, China

²School of Physics, Hangzhou Normal University, No.2318 Yuhangtang Road, Yuhang District, Hangzhou 311121, China

³Theoretical Physics Division, Institute of High Energy Physics, Chinese Academy of Sciences, 19B Yuquan Road, Shijingshan District, Beijing 100049, China

⁴School of Physics, University of Chinese Academy of Sciences, 19A Yuquan Road, Shijingshan District, Beijing 100049, China

⁵Division of Science, National Astronomical Observatory of Japan (NAOJ), and SOKENDAI, 2-21-1 Osawa, Mitaka, Tokyo 181-8588, Japan

⁶Theory Center, IPNS, and QUP (WPI), KEK, 1-1 Oho, Tsukuba, Ibaraki 305-0801, Japan

⁷Kavli IPMU (WPI), UTIAS, The University of Tokyo, Kashiwa, Chiba 277-8583, Japan

Received: date / Accepted: date

Abstract The stochastic gravitational-wave background originating from cosmic sources contains vital information about the early universe. In this work, we comprehensively study the cross-correlations between the energy-density anisotropies in scalar-induced gravitational waves (SIGWs) and the temperature anisotropies and polarization in the cosmic microwave background (CMB). In our analysis of the angular power spectra for these cross-correlations, we consider all contributions of the local-type primordial non-Gaussianity f_{NL} and g_{NL} that can lead to large anisotropies. We show that the angular power spectra are highly sensitive to primordial non-Gaussianity. Furthermore, we project the sensitivity of future gravitational-wave detectors to detect such signals and, consequently, measure the primordial non-Gaussianity.

^aCorrespondence author: wangsai@ihep.ac.cn

1 Introduction

Scalar-induced gravitational waves (SIGWs) are generated nonlinearly by the linear cosmological curvature perturbations in the early universe [1, 2, 3, 4, 5, 6, 7], with their energy-density spectrum influenced by primordial non-Gaussianity [8, 9, 10, 11, 12, 13, 14, 15]. This non-Gaussianity reflects the level of interaction of the inflaton field. Additionally, the production of SIGWs may coincide with the creation of primordial black holes (PBHs), which are considered viable candidates for dark matter [16, 17, 18]. Consequently, SIGWs serve as crucial sources of information regarding the universe's origin and evolution during a pre-recombination era that is inaccessible with other cosmological tracers, while also potentially serving as probes of dark matter. However, observations of SIGWs may face contamination from astrophysical foregrounds, such as a stochastic gravitational-wave background from compact binary coalescences [19]. Moreover, the energy-density spectrum of SIGWs exhibits degeneracy in model parameters. To address these challenges, it is essential to introduce a comprehensive set of observables that characterize SIGWs effectively.

Studies have shown that the auto-correlations among the energy-density anisotropies in SIGWs can be a valuable tool for removing astrophysical foregrounds and addressing parameter degeneracy [20, 21, 22]. It was shown that the presence of significant anisotropies in SIGWs is contingent upon the local-type primordial non-Gaussianity [23, 21, 22, 24, 25, 26, 27]. This finding underscores the potential of the angular power spectrum as a key indicator of inflation dynamics and a means to differentiate between various inflation models. It was also shown that the angular bispectra and trispectra of SIGWs are direct probes of primordial non-Gaussianity [23, 28]. However, the possible presence of parameter degeneracy, unknown systematics, and residual foregrounds in these auto-correlations highlights the need for additional observables to effectively address this challenge.

Cross-correlations between SIGWs and other cosmological tracers are being established to extract crucial information about the universe, getting rid of shortages of the auto-correlations. Recent analyses have investigated the cross-correlations between the energy-density anisotropies in SIGWs and the temperature anisotropies in the cosmic microwave background (CMB) [29, 30, 31]. These cross-correlations can be significant due to the shared origin of both anisotropies and the common influence of large-scale density perturbations on the propagation of gravitons and photons. Future advancements in gravitational-wave detectors and CMB experiments are poised to offer precise constraints on the non-Gaussian parameters through these cross-correlations [32, 33, 34]. Therefore, the integration of both auto- and cross-correlations would enhance our comprehension of the early universe.

In this study, we conduct a comprehensive investigation into the cross-correlations between SIGWs and the CMB. Our analysis encompasses the influence of local-type primordial non-Gaussianity, parameterized as f_{NL} and g_{NL} , on the energy density of

SIGWs at both background and anisotropy levels [22]. We also examine the cross-correlations involving polarization in the CMB, besides temperature anisotropies. Furthermore, we demonstrate that the parameter degeneracy can be resolved by taking into account these cross-correlations. Through the application of the Fisher-matrix method, we evaluate the sensitivity of future gravitational-wave detectors and CMB experiments in detecting these signals and accurately measuring the non-Gaussian parameters.

The remaining of the paper is arranged as follows. By briefly summarizing the formulas for the energy-density anisotropies in SIGWs, we provide the formulas for the cross-correlations between SIGWs and the CMB in Section 2. We perform the Fisher-matrix forecastings for the non-Gaussian parameter f_{NL} in Section 3. We demonstrate the conclusions and discussion in Section 4.

2 Cross-correlations between SIGWs and the CMB

In this section, we provide a brief overview of the fundamental formulas, with more comprehensive details available in Ref. [22].

2.1 Temperature anisotropies and polarization in the CMB

Considerable research has been dedicated to investigating temperature anisotropies and polarization in the CMB [35,36,37]. Photons from the early universe follow a thermal distribution resembling a blackbody spectrum. Inhomogeneities in the energy density of these relic photons result in temperature fluctuations, which are observed as temperature anisotropies in the CMB. Additionally, the presence of a quadrupole moment gives rise to polarization signals within the CMB. In this section, we present the formulas for temperature anisotropies (T) and polarization (E), excluding the consideration of B-mode polarization due to its lack of correlation with SIGWs resulting from parity constraints.

The standard practice is to express the T and E modes of the CMB in harmonic space, where the coefficients of spherical harmonics are denoted as

$$a_{X\ell m} = 4\pi(-i)^\ell \int \frac{d^3\mathbf{k}}{(2\pi)^3} e^{i\mathbf{k}\cdot\mathbf{x}_0} Y_{\ell m}^*(\hat{\mathbf{k}}) \mathcal{R}(\mathbf{k}) \Delta_{X\ell}(k, \eta_0), \quad (1)$$

where \mathcal{R} represents the primordial curvature perturbations, \mathbf{k} denotes the wavevector of these perturbations with $\hat{\mathbf{k}}$ indicating its direction, and $\Delta_{X\ell}$ corresponds to the transfer function of X (either T or E). Typically, the determination of $\Delta_{X\ell}$ involves solving the Boltzmann-Einstein equations, a task often performed using the publicly accessible CLASS¹ software [38].

¹https://github.com/lesgourg/class_public

The angular power spectrum of the CMB is defined as

$$\langle a_{X\ell m} a_{X'\ell' m'}^* \rangle = \delta_{\ell\ell'} \delta_{mm'} C_\ell^{XX'} , \quad (2)$$

for which we have assumed the cosmological principle. It is explicitly shown as

$$C_\ell^{XX'} = 4\pi \int d \ln k \Delta_X(k, \eta_0) \Delta_{X'}(k, \eta_0) P_L(k) , \quad (3)$$

where P_L represents the dimensionless power spectrum of \mathcal{R} at large scales. For simplicity, we assume that the spectral tilt vanishes, i.e., [39,40]

$$P_L(k) = A_L , \quad (4)$$

where A_L represents the spectral amplitude. However, it can be extended to accommodate other spectral tilts if necessary. In this study, the subscript $_0$ denotes cosmological quantities in the present-day cosmos, with detailed values provided in Ref. [41].

2.2 Average background and the energy-density anisotropies in SIGWs

In contrast to relic photons, gravitons are intrinsically non-thermal. It is crucial to comprehend the energy-density spectrum of SIGWs before delving into the incorporation of energy-density fluctuations, which can manifest as energy-density anisotropies within SIGWs. While gravitons and relic photons travel along similar geodesics, the origins of energy-density anisotropies in SIGWs do not perfectly align with temperature anisotropies in the CMB. This discrepancy stems from the nonlinear production of SIGWs by linear cosmological curvature perturbations, necessitating the consideration of non-adiabatic initial conditions instead of the adiabatic conditions typically assumed for the CMB. Such initial conditions can lead to significant anisotropies in SIGWs in principle.

2.2.1 Average background

The energy-density (fraction) spectrum of SIGWs at the average background level has been comprehensively investigated in Refs. [22,42,26] by considering the local-type primordial non-Gaussianity parameters f_{NL} and g_{NL} . In this work, by saying ‘‘average background’’, we mean the monopole, i.e., isotropic component of the SGWB, which is denoted by $\bar{\Omega}_{\text{gw}}$. Additional studies on this topic are available in Refs. [21,24,43,44,45,46,25,47,48,49,50,51,52,53,54,55,56,57,58,47,48,25,59,60]. In our approach, we utilize diagrammatic techniques to derive semi-analytical formulas

for this spectrum, as detailed in Ref. [22]. Specifically, the energy-density spectrum is expressed as

$$\begin{aligned} \Omega_{\text{gw}}(\eta_i, q) = & \Omega_{\text{gw}}^{(0,0)} + \Omega_{\text{gw}}^{(0,1)} + \Omega_{\text{gw}}^{(1,0)} + \Omega_{\text{gw}}^{(0,2)} + \Omega_{\text{gw}}^{(1,1)} \\ & + \Omega_{\text{gw}}^{(2,0)} + \Omega_{\text{gw}}^{(0,3)} + \Omega_{\text{gw}}^{(1,2)} + \Omega_{\text{gw}}^{(0,4)}, \end{aligned} \quad (5)$$

where η_i signifies the production time of SIGWs, q is the gravitational-wave wavenumber, and the expressions for $\Omega_{\text{gw}}^{(a,b)}$ are sufficiently complex to make listing them in this paper impractical, but their semi-analytic results can be found in Fig. 5 of Ref. [22]. Regarding perturbations that produce SIGWs, we consider the dimensionless power spectrum of \mathcal{R} at small scales to be

$$P_S(k) = \frac{A_S}{\sqrt{2\pi}\sigma^2} \exp\left[-\frac{\ln^2(k/k_p)}{2\sigma^2}\right], \quad (6)$$

where A_S and σ represent the spectral amplitude and width, with $k_p = 2\pi f_p$ denoting the peak wavenumber with f_p being the peak frequency. Assuming $\sigma = 1$, we graphically represented $\Omega_{\text{gw}}^{(a,b)}$ as a function of q in Fig. 5 of Ref. [22] for clarity.

Ultimately, we derive the energy-density spectrum of SIGWs in the present-day universe as

$$\Omega_{\text{gw},0}(\nu) \simeq \Omega_{r,0} \Omega_{\text{gw}}(\eta_i, q), \quad (7)$$

where $\Omega_{r,0} = 4.2 \times 10^{-5} h^{-2}$, with h representing the dimensionless Hubble constant, denotes the energy-density fraction of radiation in the present-day universe, and $\nu = q/(2\pi)$ is the gravitational-wave frequency. In the above equation, we neglect contributions from effective relativistic species during the thermal evolution of the early universe, which can be reintroduced if required. Assuming $\sigma = 1$, we presented illustrations of $\Omega_{\text{gw},0}$ as a function of ν in Fig. 6 of Ref. [22] for clarity.

2.2.2 Energy-density anisotropies

The investigation of energy-density anisotropies in SIGWs has recently been explored in Refs. [23, 21, 61, 62, 20, 63, 64, 32, 65, 66, 24, 22, 25, 28, 30, 27]. Specifically, we presented all contributions of f_{NL} and g_{NL} to these anisotropies in Refs. [22]. Similar to the CMB, the energy-density fluctuations of SIGWs can also be described in harmonic space. The coefficients of spherical harmonics are provided as

$$\delta_{\ell m} = 4\pi(-i)^\ell \int \frac{d^3\mathbf{k}}{(2\pi)^3} e^{i\mathbf{k}\cdot\mathbf{x}_0} Y_{\ell m}^*(\hat{\mathbf{k}}) \mathcal{R}(\mathbf{k}) \mathcal{T}_\ell(q, k, \eta_0). \quad (8)$$

Here, the transfer function \mathcal{T}_ℓ can be derived by solving the Boltzmann-Einstein equations [67, 23]. According to Ref. [22], we explicitly represent it as

$$\begin{aligned} \mathcal{T}_\ell = \frac{\Omega_{\text{gw},0}}{4\pi} \left\{ \left(\frac{\Omega_{\text{ng}}}{\Omega_{\text{gw}}} \right) j_\ell(k(\eta_0 - \eta_i)) + (4 - n_{\text{gw}}) T_\psi(\eta_i, k) j_\ell(k(\eta_0 - \eta_i)) \right. \\ \left. + (4 - n_{\text{gw}}) \int_{\eta_i}^{\eta_0} d\eta \left(\frac{\partial T_\phi(\eta, k)}{\partial \eta} + \frac{\partial T_\psi(\eta, k)}{\partial \eta} \right) j_\ell(k(\eta_0 - \eta)) \right\} \quad (9) \end{aligned}$$

where the tilt of energy-density spectrum is defined as $n_{\text{gw}}(\nu) = d \ln \Omega_{\text{gw},0}(\nu) / d \ln \nu$, Ω_{ng} denotes all terms involving the couplings of long- and short-wavelength perturbations, T_ψ and T_ϕ represent the transfer functions of scalar perturbations in the comoving Newtonian gauge, and $j_\ell(x)$ is the spherical Bessel function. In this study, we utilize energy-density fluctuations instead of energy-density contrasts. The latter are defined as the former divided by the energy density per solid angle of the average background. This convention results in a factor of $\Omega_{\text{gw},0}/(4\pi)$ in Eq. (9). We represent Ω_{ng} as

$$\begin{aligned} \Omega_{\text{ng}}(\eta_i, q) = & \frac{6f_{\text{NL}}}{5} (4\Omega_{\text{gw}}^{(0,0)} + 3\Omega_{\text{gw}}^{(0,1)} + 2\Omega_{\text{gw}}^{(1,0)} + 2\Omega_{\text{gw}}^{(0,2)} + \Omega_{\text{gw}}^{(1,1)} + \Omega_{\text{gw}}^{(0,3)}) \\ & + \frac{9g_{\text{NL}}}{5f_{\text{NL}}} (2\Omega_{\text{gw}}^{(1,0)} + 2\Omega_{\text{gw}}^{(1,1)} + 4\Omega_{\text{gw}}^{(2,0)} + 2\Omega_{\text{gw}}^{(1,2)}) , \end{aligned} \quad (10)$$

which aligns with Eq. (3.14) in Ref. [22]. In Eq. (9), the first term on the right-hand side represents the initial inhomogeneities, while the second and third terms correspond to the Sachs-Wolfe (SW) and integrated Sachs-Wolfe (ISW) effects [68]. The latter two effects are similar to those observed in the CMB.

It is important to highlight that the non-adiabatic initial conditions differ from the adiabatic initial conditions assumed for the CMB. When we consider a large $|f_{\text{NL}}|$ value, this distinct initial condition is responsible for the significant anisotropies in SIGWs.

In order to characterize the auto-correlations of energy-density anisotropies (G) in SIGWs, the angular power spectrum is defined as

$$\langle \delta_{\ell m} \delta_{\ell' m'}^* \rangle = \delta_{\ell \ell'} \delta_{m m'} C_\ell^{\text{GG}} , \quad (11)$$

leading to the following expression

$$C_\ell^{\text{GG}} = 4\pi \int d \ln k \mathcal{T}_\ell^2(q, k, \eta_0) P_L(k) . \quad (12)$$

In Fig. 1, we present numerical results showcasing the auto-correlations of SIGWs, characterized by a flat angular power spectrum. We show the 1σ uncertainty due to cosmic variance (CV), namely $\Delta C_\ell = \sqrt{2/(2\ell + 1)} C_\ell$, in shaded regions. Here, we focus on the auto-correlations within the same frequency band of gravitational waves. However, our research methodology can be readily extended to study correlations between different frequency bands, as demonstrated in Refs. [21, 22, 30]. Based on Fig. 1, we also illustrate that the auto-correlation spectrum exhibits significant degeneracy in model parameters, as discussed in Refs. [21, 22]. In Fig. 2, we demonstrate how auto-correlations vary with different frequency bands by considering a given angular multipole moment, i.e., $\ell = 4$. Such dependence would be important to extracting vital information by performing the component separation [69, 70].

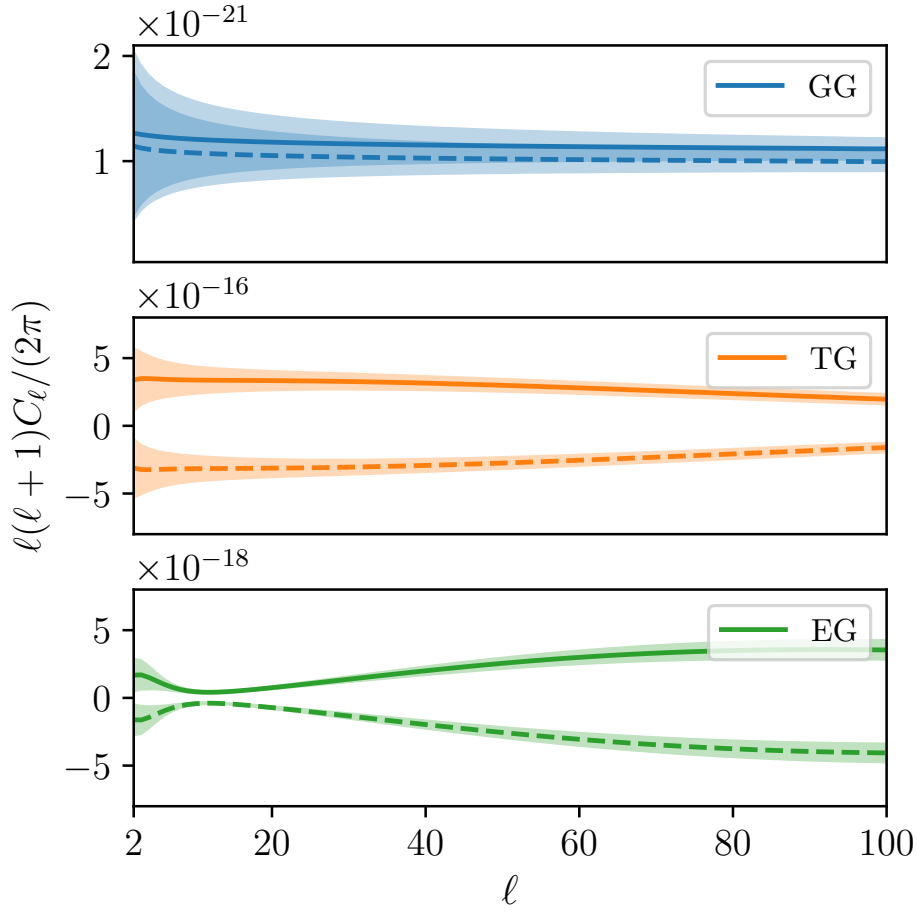


Fig. 1: The angular power spectra for the auto- and cross-correlations are shown with CV shaded. For illustration, we depict them in the frequency band of $\nu = f_p$ by assuming the model parameters $A_S = 0.02$, $\sigma = 1$, $f_{\text{NL}} = \pm 10$ (plus in solid while minus in dashed), and $g_{\text{NL}} = 20$. The shaded region shows the $\pm 1\sigma$ (68% C.L.) uncertainty from CV only.

2.3 Cross-correlations between SIGWs and the CMB

The angular power spectrum for cross-correlations between SIGWs and the CMB is defined as

$$\frac{1}{2} \langle a_{\chi \ell m} \delta_{\ell' m'}^* + a_{\chi \ell m}^* \delta_{\ell' m'} \rangle = \delta_{\ell \ell'} \delta_{m m'} C_{\ell}^{\text{XG}}, \quad (13)$$

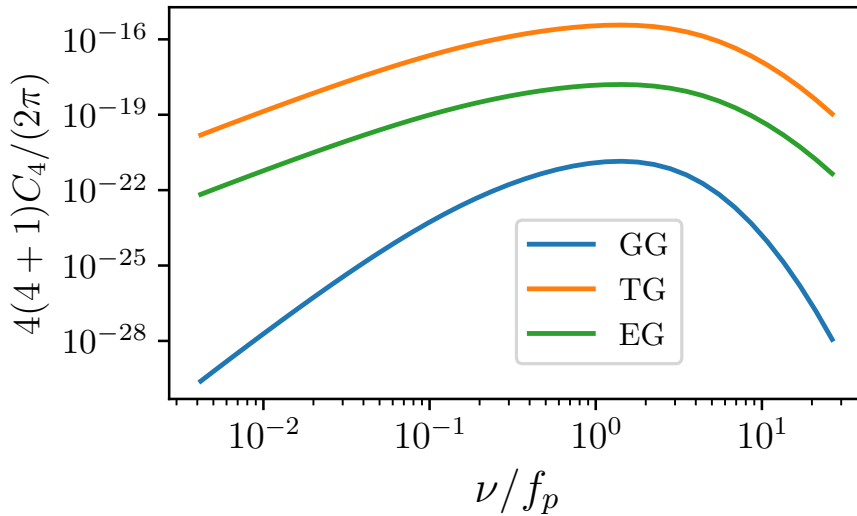


Fig. 2: We show dependence of the angular power spectra on frequency bands. For the purpose of illustration, we fix $\ell = 4$ and the model parameters $A_S = 0.02$, $\sigma = 1$, $f_{\text{NL}} = 10$, and $g_{\text{NL}} = 20$.

where the superscript XG indicates the cross-correlations between X-mode of the CMB and the energy-density anisotropies in SIGWs. This is explicitly expressed as

$$C_\ell^{\text{XG}} = 4\pi \int d \ln k \Delta_{X\ell}(k, \eta_0) \mathcal{T}_\ell(q, k, \eta_0) P_L(k), \quad (14)$$

which stands as one of the key outcomes of our current study. This result will be used to estimate the projected sensitivity of future experiments to our model parameters in the subsequent section. We also illustrate numerical results for the cross-correlations in Fig. 1 and their dependence on frequency bands in Fig. 2. Our analysis reveals that the angular power spectra for cross-correlations exhibit a nearly flat profile, with certain features being introduced by the CMB. Based on Fig. 1, we observe that the cross-correlation spectra can alleviate the degeneracy in model parameters, potentially enabling the extraction of model information. That is, cross-correlation spectra can help distinguish between positive and negative values of f_{NL} . In addition, we expect that they exhibit dependence on frequency bands. Based on our analysis outlined in this section, we expect that a combination of auto- and cross-correlations would be useful to subtracting systematics and foregrounds from observations by using, e.g., component separation [69,70]. We would leave such analysis to future works, as they are outside the scope of our current work.

3 Fisher-matrix forecastings

In this section, utilizing the Fisher-matrix approach ² [72], we investigate the precision of measuring model parameters by detecting the cross-correlations between SIGWs and the CMB using upcoming gravitational-wave detection. For the purpose of illustration, our focus is solely on the non-linear parameter f_{NL} , and thereby let $g_{\text{NL}} = 0$. Nevertheless, our research methodology can be readily extended to encompass other model parameters as required. Throughout this work, we do not consider potential sources of astrophysical foregrounds, which are left to be studied by future works.

The signal-to-noise ratio (SNR) for a combination of auto- and cross-correlations is defined as

$$\text{SNR}^2 = \sum_{\ell=2}^{\ell_{\text{max}}} \mathbf{C}^T \mathbf{C}^{-1} \mathbf{C}, \quad (15)$$

where we define $\mathbf{C} = (C_\ell^{\text{GG}}, C_\ell^{\text{TG}}, C_\ell^{\text{EG}})^T$, and the covariance matrix is represented as ³

$$\mathbf{C} = \begin{pmatrix} \sigma_\ell^{\text{GG-GG}^2} & \sigma_\ell^{\text{GG-TG}^2} & \sigma_\ell^{\text{GG-EG}^2} \\ \sigma_\ell^{\text{GG-TG}^2} & \sigma_\ell^{\text{TG-TG}^2} & \sigma_\ell^{\text{TG-EG}^2} \\ \sigma_\ell^{\text{GG-EG}^2} & \sigma_\ell^{\text{TG-EG}^2} & \sigma_\ell^{\text{EG-EG}^2} \end{pmatrix}. \quad (17)$$

Our analysis includes the noise characteristics N_ℓ of gravitational-wave detectors ⁴, while considering only CV for the CMB since the noise in future CMB experiments

²Ref. [71] introduced a Bayesian approach, which could be applied to our current study in principle. Nevertheless, for illustrative purposes, we anticipate that the Fisher-matrix approach will be adequate for our theoretical analysis.

³Elements of \mathbf{C} are specifically given as

$$\sigma_\ell^{\text{GG-GG}^2} = \frac{2}{2\ell+1} (C_\ell^{\text{GG}} + N_\ell)^2, \quad (16a)$$

$$\sigma_\ell^{\text{GG-TG}^2} = \frac{2}{2\ell+1} [(C_\ell^{\text{GG}} + N_\ell) C_\ell^{\text{TG}}], \quad (16b)$$

$$\sigma_\ell^{\text{GG-EG}^2} = \frac{2}{2\ell+1} [(C_\ell^{\text{GG}} + N_\ell) C_\ell^{\text{EG}}], \quad (16c)$$

$$\sigma_\ell^{\text{TG-TG}^2} = \frac{1}{2\ell+1} [(C_\ell^{\text{TG}})^2 + C_\ell^{\text{TT}} (C_\ell^{\text{GG}} + N_\ell)], \quad (16d)$$

$$\sigma_\ell^{\text{TG-EG}^2} = \frac{1}{2\ell+1} [C_\ell^{\text{TE}} (C_\ell^{\text{GG}} + N_\ell) + C_\ell^{\text{TG}} C_\ell^{\text{EG}}], \quad (16e)$$

$$\sigma_\ell^{\text{EG-EG}^2} = \frac{1}{2\ell+1} [(C_\ell^{\text{EG}})^2 + C_\ell^{\text{EE}} (C_\ell^{\text{GG}} + N_\ell)]. \quad (16f)$$

⁴We use the North American Nanohertz Observatory for Gravitational Waves (NANOGrav) [73], Laser Interferometer Space Antenna (LISA) [74, 75], Big Bang Observer (BBO) [76, 77], Deci-hertz Interferometer Gravitational wave Observatory (DECIGO) [78, 79], and a network of Einstein Telescope (ET) [80] and Cosmic Explorer (CE) [81]. We utilize the noise from the most sensitive frequency band for each detector [82, 83]. We depict them in Fig. 3 to compare with the specified signal. Similar methodologies can be applied to analyze other detectors.

could potentially be dominated by CV. When ignoring N_ℓ , we obtain an inevitable uncertainty due to CV.

To evaluate the precision of measuring model parameters, we utilize the Fisher matrix, denoted as F , for which detailed derivations have been explicitly shown in Refs. [33, 84]. Its components are given by

$$\begin{aligned} F_{ij} &= \sum_{\ell}^{\ell_{\max}} \frac{2\ell + 1}{2} \text{Tr} \left[\frac{\partial C_\ell}{\partial \theta_i} C_\ell^{-1} \frac{\partial C_\ell}{\partial \theta_j} C_\ell^{-1} \right] \\ &= \sum_{\ell}^{\ell_{\max}} \frac{\partial \mathbf{C}^T}{\partial \theta_i} \mathbf{C}^{-1} \frac{\partial \mathbf{C}}{\partial \theta_j}, \end{aligned} \quad (18)$$

where $\partial \mathbf{C} / \partial \theta$ denotes the derivative of each element of \mathbf{C} , as defined below Eq. (15), with respect to a model parameter θ , \mathbf{C} is the covariance matrix, as defined in Eq. (17), and ℓ_{\max} represents the maximum value of angular multipole moments that are relevant for a given detector. For the sake of clarity, we concentrate on a single parameter, specifically $p_1 = f_{\text{NL}}$. The 1σ uncertainty of f_{NL} is determined by the Cramér-Rao bound, i.e.,

$$\sigma_{f_{\text{NL}}} = \sqrt{(F^{-1})_{11}}, \quad (19)$$

which provides a rough estimate of the measurement precision. This level of analysis is adequate for our theoretical investigation.

To assess the performance of detectors in measuring auto- and cross-correlations, we present the SNRs as a function of ℓ_{\max} in Fig. 4. In this analysis, we assume $f_{\text{NL}} = 10$, $g_{\text{NL}} = 0$, $A_S = 0.02$, $\sigma = 1$, and $f_p = f_*$, where f_* represents the frequency associated with the optimal sensitivity of detectors. We examine two scenarios: one focusing solely on auto-correlations and the other involving a combination of auto- and cross-correlations. Our findings reveal that the inclusion of cross-correlations consistently improves the SNR compared to the auto-correlation-only scenario. Nevertheless, the SNR for both cases potentially reaches a saturation point with increasing ℓ_{\max} due to the limitations in detectors' angular resolution. Additionally, we present the CV limits for comparison. For the specified signal, DE-CIGO can achieve the CV limits as its noise level is significantly lower than CV. Conversely, other detectors are able to approach the CV limits only at the lowest angular multipole moments.

To assess the precision of parameter estimation for the model, we analyze the uncertainties in f_{NL} measured by the detectors under consideration in Fig. 5. We use $\ell_{\max} = 6$ for NANOGrav [82] while $\ell_{\max} = 30$ for others [83]. We examine the same two cases as depicted in Fig. 4, but for each f_{NL} value, we determine A_S by setting $\text{SNR} = 1$ in the auto-correlation-only case. For the specified signal, we observe that the combination of auto- and cross-correlations yields reduced uncertainties in estimating this parameter compared to the case focusing solely on auto-correlations. By increasing the SNR, these uncertainties can be proportionally reduced.

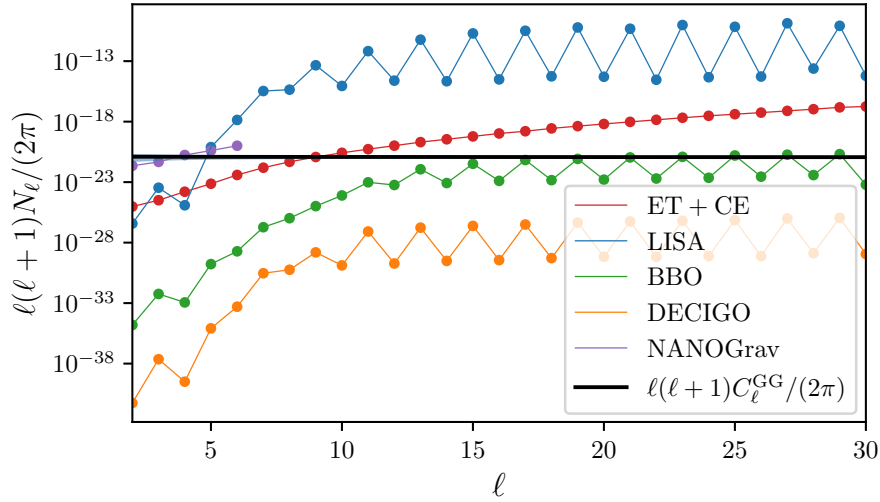


Fig. 3: Comparison between the signal and the optimal sensitivity of detectors. The noise level of NANOGrav is illustrated as the lowest in the lower panel of Fig. 4 in Ref. [82], while the noise levels of other detectors are depicted in Fig. 7 of Ref. [83]. In our analysis, we consider a set of model parameters $f_{\text{NL}} = 10$, $g_{\text{NL}} = 0$, $A_S = 0.02$, $\sigma = 1$, and $f_p = f_*$ with f_* being the frequency associated with the optimal sensitivity. For the signal, we utilize the specified auto-correlated angular power spectrum at $\nu = f_p$.

4 Conclusions and discussion

Our study focused on exploring the cross-correlation between the energy-density anisotropies in SIGWs and the temperature anisotropies and polarization in the CMB. We derived the expressions for the corresponding angular power spectra and integrated them as template banks into our customized version of `GW_CLASS`. It is worth noting that our analysis accounted for all contributions stemming from the local-type primordial non-Gaussian parameters f_{NL} and g_{NL} , which have the potential to significantly alter the existing findings in the literature. We suggested that the distinct dependencies of the angular power spectra on model parameters could prove instrumental in resolving degeneracies within these parameters. Furthermore, we determined the projected sensitivity of multi-band gravitational-wave detectors and CMB experiments in detecting these signals and precisely measuring our model parameters, especially those related to primordial non-Gaussianity. We anticipate that the combination of auto- and cross-correlations will enrich our understanding of the early universe.

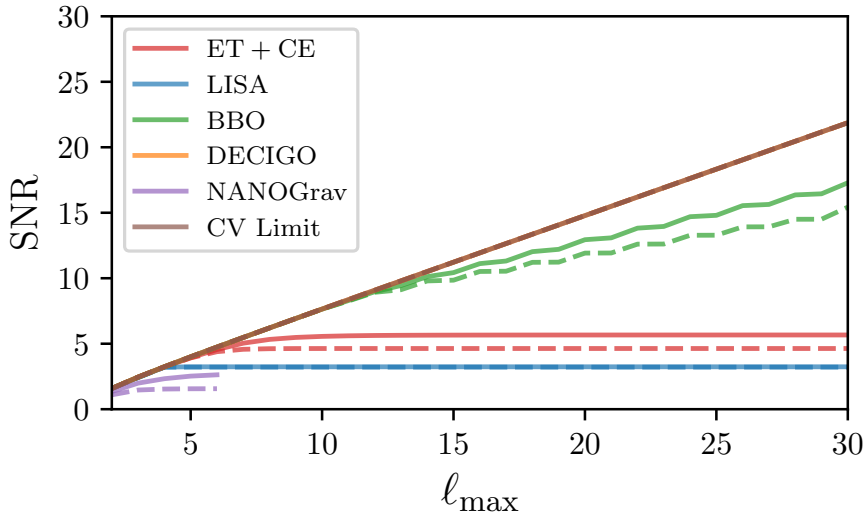


Fig. 4: The SNRs are depicted for the detection of auto-correlations (dashed curves) and both auto- and cross-correlations (solid curves) using future gravitational-wave detectors. We adopt the same set of model parameters as those in Fig. 3. For comparison, we include the CV limits. It is worth noting that the curves corresponding to DECIGO perfectly align with the CV limits.

The energy-density anisotropies in SIGWs may have origins partially attributed to the SW and ISW effects, akin to those observed in the CMB but with subtle distinctions. Gravitons were generated before the radiation-matter equality epoch and traversed longer distances compared to the last scattering of photons. In contrast to the CMB, SIGWs are additionally influenced by contributions from effective relativistic species and the early ISW effect predating the recombination era. In our present investigation, we considered these effects by utilizing the modified version of `GW.CLASS`. Our findings indicate that the anisotropies in SIGWs stemming from these effects are at a level of approximately $\sim 10^{-4}$, which is comparable to the $\sim 10^{-5}$ level observed in the CMB [41]. Furthermore, it is important to acknowledge that the SW and ISW effects are independent of specific models and are inherent in the observations.

The initial inhomogeneities in SIGWs are inherent to the system and contingent on the specific production mechanism, thus encapsulating information about the underlying model. In our current study, we consider the non-adiabatic initial conditions that have been extensively explored in our previous works. Unlike the CMB, the significant anisotropies in SIGWs can be attributed to these initial conditions, particularly in the presence of local-type primordial non-Gaussianity. In such scenar-

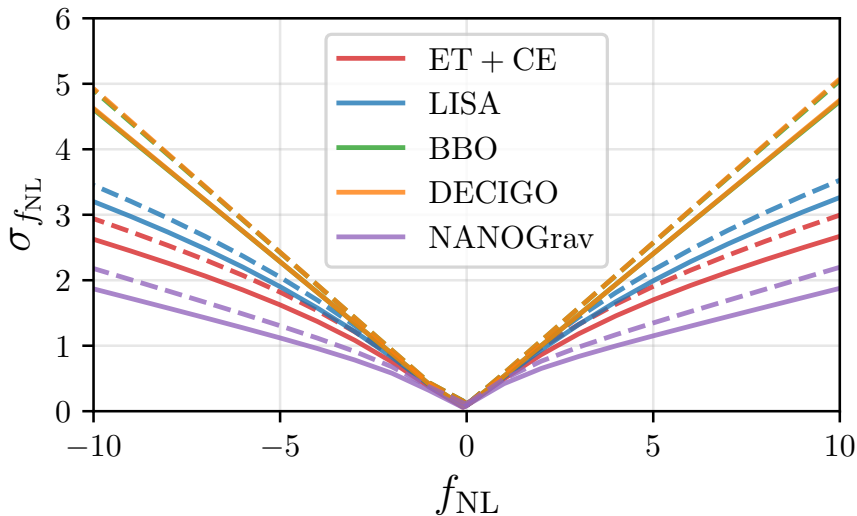


Fig. 5: The uncertainties in f_{NL} are assessed by measuring the auto-correlations (dashed curves) and both auto- and cross-correlations (solid curves) using prospective gravitational-wave detectors. We use $\ell_{\text{max}} = 6$ for NANOGrav while $\ell_{\text{max}} = 30$ for others. For each f_{NL} value, we calculate A_S setting $\text{SNR} = 1$ in the auto-correlation-only case, while assuming $g_{\text{NL}} = 0$, $\sigma = 1$, and $f_p = f_*$.

ios, it is anticipated that short-wavelength modes will interact with long-wavelength modes, with the former nonlinearly generating SIGWs. Consequently, the spatial distribution of energy density in SIGWs is influenced by the modulation induced by the latter.

We derived the angular power spectra for the auto- and cross-correlations, revealing their strong dependence on the level of primordial non-Gaussianity. On the one hand, we may be capable of differentiating SIGWs from astrophysical foregrounds by examining the distinctive features present in their angular power spectra. Specifically, the angular power spectra of SIGWs exhibit characteristic scalings of $\ell(\ell+1)C_\ell \sim \ell^0$, in contrast to those of SGWB originating from binary black holes which roughly follow $\ell(\ell+1)C_\ell \sim \ell^1$ [85, 86, 87, 88, 89, 90, 91, 67, 92, 93, 94, 95]. This disparity in scaling suggests the potential to distinguish between these two signal components based on their angular power spectrum characteristics [20, 96, 97]. On the other hand, our findings indicated that combining the cross-correlation spectra can alleviate the parameter degeneracy observed in the auto-correlation spectrum. This outcome has the potential to distinguish between various models of inflation. Therefore, our investigation may pave the way for novel approaches to measure non-Gaussian parameters and, consequently, delve into the origins and early evolution of the universe.

We delved deeper into exploring the anticipated sensitivity of forthcoming multi-band gravitational-wave detectors in measuring model parameters, specifically focusing on the non-Gaussian parameter f_{NL} . Our analysis revealed that the combined consideration of both auto- and cross-correlated angular power spectra could effectively enhance precision in parameter measurements. Furthermore, we identified the inherent limitations on the precision of these measurements stemming from CV.

We should emphasize that we have assumed scale-invariant local-type primordial non-Gaussianity across the wide range of scales connecting CMB/SIGW anisotropy (large angular scales) to the much smaller physical scales set by gravitational-wave frequencies. Accordingly, we expect that our constraints do not apply to models with strongly scale-dependent $f_{\text{NL}}(k)$, which are left to investigate by future works.

Our research methodology can be extended to investigate cross-correlations between SIGWs (or other sources of SGWB) and other cosmological probes such as large-scale structures (LSS), hydrogen 21 cm lines, etc. However, we defer these investigations to future works as they fall outside the scope of our present research.

Acknowledgements S.W. and J.P.L. are supported by the National Key R&D Program of China No. 2023YFC2206403 and the National Natural Science Foundation of China (Grant No. 12175243). Z.C.Z. is supported by the National Key Research and Development Program of China Grant No. 2021YFC2203001. K.K. is supported by KAKENHI Grant Nos. JP22H05270, JP23KF0289, JP24H01825, JP24K07027. This work is supported by the High-performance Computing Platform of China Agricultural University.

References

1. K.N. Ananda, C. Clarkson, D. Wands, *Phys. Rev. D* **75**, 123518 (2007). DOI 10.1103/PhysRevD.75.123518
2. D. Baumann, P.J. Steinhardt, K. Takahashi, K. Ichiki, *Phys. Rev. D* **76**, 084019 (2007). DOI 10.1103/PhysRevD.76.084019
3. J.R. Espinosa, D. Racco, A. Riotto, *JCAP* **09**, 012 (2018). DOI 10.1088/1475-7516/2018/09/012
4. K. Kohri, T. Terada, *Phys. Rev. D* **97**(12), 123532 (2018). DOI 10.1103/PhysRevD.97.123532
5. S. Mollerach, D. Harari, S. Matarrese, *Phys. Rev. D* **69**, 063002 (2004). DOI 10.1103/PhysRevD.69.063002
6. H. Assadullahi, D. Wands, *Phys. Rev. D* **81**, 023527 (2010). DOI 10.1103/PhysRevD.81.023527
7. G. Domènech, *Universe* **7**(11), 398 (2021). DOI 10.3390/universe7110398
8. J.M. Maldacena, *JHEP* **05**, 013 (2003). DOI 10.1088/1126-6708/2003/05/013
9. N. Bartolo, E. Komatsu, S. Matarrese, A. Riotto, *Phys. Rept.* **402**, 103 (2004). DOI 10.1016/j.physrep.2004.08.022
10. T.J. Allen, B. Grinstein, M.B. Wise, *Phys. Lett. B* **197**, 66 (1987). DOI 10.1016/0370-2693(87)90343-1
11. N. Bartolo, S. Matarrese, A. Riotto, *Phys. Rev. D* **65**, 103505 (2002). DOI 10.1103/PhysRevD.65.103505

-
12. V. Acquaviva, N. Bartolo, S. Matarrese, A. Riotto, Nucl. Phys. B **667**, 119 (2003). DOI 10.1016/S0550-3213(03)00550-9
 13. F. Bernardeau, J.P. Uzan, Phys. Rev. D **66**, 103506 (2002). DOI 10.1103/PhysRevD.66.103506
 14. X. Chen, M.x. Huang, S. Kachru, G. Shiu, JCAP **01**, 002 (2007). DOI 10.1088/1475-7516/2007/01/002
 15. C.T. Byrnes, K.Y. Choi, Adv. Astron. **2010**, 724525 (2010). DOI 10.1155/2010/724525
 16. B. Carr, F. Kuhnel, Ann. Rev. Nucl. Part. Sci. **70**, 355 (2020). DOI 10.1146/annurev-nucl-050520-125911
 17. B. Carr, K. Kohri, Y. Sendouda, J. Yokoyama, Rept. Prog. Phys. **84**(11), 116902 (2021). DOI 10.1088/1361-6633/ac1e31
 18. B. Carr, S. Clesse, J. Garcia-Bellido, M. Hawkins, F. Kuhnel, Phys. Rept. **1054**, 1 (2024). DOI 10.1016/j.physrep.2023.11.005
 19. T. Regimbau, Res. Astron. Astrophys. **11**, 369 (2011). DOI 10.1088/1674-4527/11/4/001
 20. N. Bartolo, et al., JCAP **11**, 009 (2022). DOI 10.1088/1475-7516/2022/11/009
 21. J.P. Li, S. Wang, Z.C. Zhao, K. Kohri, JCAP **10**, 056 (2023). DOI 10.1088/1475-7516/2023/10/056
 22. J.P. Li, S. Wang, Z.C. Zhao, K. Kohri, JCAP **06**, 039 (2024). DOI 10.1088/1475-7516/2024/06/039
 23. N. Bartolo, D. Bertacca, V. De Luca, G. Franciolini, S. Matarrese, M. Peloso, A. Ricciardone, A. Riotto, G. Tasinato, JCAP **02**, 028 (2020). DOI 10.1088/1475-7516/2020/02/028
 24. S. Wang, Z.C. Zhao, J.P. Li, Q.H. Zhu, Phys. Rev. Res. **6**(1), L012060 (2024). DOI 10.1103/PhysRevResearch.6.L012060
 25. Y.H. Yu, S. Wang, Phys. Rev. D **109**(8), 083501 (2024). DOI 10.1103/PhysRevD.109.083501
 26. J.Á. Ruiz, J. Rey, JCAP **04**, 026 (2025). DOI 10.1088/1475-7516/2025/04/026
 27. J. Rey, (2024). DOI 10.48550/arXiv.2411.08873
 28. J.P. Li, S. Wang, Z.C. Zhao, K. Kohri, JCAP **05**, 109 (2024). DOI 10.1088/1475-7516/2024/05/109
 29. E. Dimastrogiovanni, M. Fasiello, A. Malhotra, G. Tasinato, JCAP **01**, 018 (2023). DOI 10.1088/1475-7516/2023/01/018
 30. F. Schulze, L. Valbusa Dall'Armi, J. Lesgourgues, A. Ricciardone, N. Bartolo, D. Bertacca, C. Fidler, S. Matarrese, JCAP **10**, 025 (2023). DOI 10.1088/1475-7516/2023/10/025
 31. R.G. Cai, S.J. Wang, Z.Y. Yuwen, X.X. Zeng, JCAP **01**, 011 (2025). DOI 10.1088/1475-7516/2025/01/011
 32. A. Malhotra, E. Dimastrogiovanni, M. Fasiello, M. Shiraishi, JCAP **03**, 088 (2021). DOI 10.1088/1475-7516/2021/03/088
 33. G. Perna, A. Ricciardone, D. Bertacca, S. Matarrese, JCAP **10**, 014 (2023). DOI 10.1088/1475-7516/2023/10/014
 34. P. Adshead, N. Afshordi, E. Dimastrogiovanni, M. Fasiello, E.A. Lim, G. Tasinato, Phys. Rev. D **103**(2), 023532 (2021). DOI 10.1103/PhysRevD.103.023532
 35. U. Seljak, M. Zaldarriaga, Astrophys. J. **469**, 437 (1996). DOI 10.1086/177793
 36. M. Zaldarriaga, U. Seljak, Phys. Rev. D **55**, 1830 (1997). DOI 10.1103/PhysRevD.55.1830
 37. M. Kamionkowski, A. Kosowsky, A. Stebbins, Phys. Rev. D **55**, 7368 (1997). DOI 10.1103/PhysRevD.55.7368
 38. D. Blas, J. Lesgourgues, T. Tram, Journal of Cosmology and Astroparticle Physics **2011**(07), 034-034 (2011). DOI 10.1088/1475-7516/2011/07/034. URL <http://dx.doi.org/10.1088/1475-7516/2011/07/034>
 39. J.Q. Jiang, Y.S. Piao, Phys. Rev. D **105**(10), 103514 (2022). DOI 10.1103/PhysRevD.105.103514

-
40. G. Ye, J.Q. Jiang, Y.S. Piao, *Phys. Rev. D* **106**(10), 103528 (2022). DOI 10.1103/PhysRevD.106.103528
 41. N. Aghanim, et al., *Astron. Astrophys.* **641**, A6 (2020). DOI 10.1051/0004-6361/201833910. [Erratum: *Astron. Astrophys.* 652, C4 (2021)]
 42. C. Yuan, D.S. Meng, Q.G. Huang, *JCAP* **12**, 036 (2023). DOI 10.1088/1475-7516/2023/12/036
 43. T. Nakama, J. Silk, M. Kamionkowski, *Phys. Rev. D* **95**(4), 043511 (2017). DOI 10.1103/PhysRevD.95.043511
 44. J. Garcia-Bellido, M. Peloso, C. Unal, *JCAP* **09**, 013 (2017). DOI 10.1088/1475-7516/2017/09/013
 45. P. Adshead, K.D. Lozanov, Z.J. Weiner, *JCAP* **10**, 080 (2021). DOI 10.1088/1475-7516/2021/10/080
 46. H.V. Ragavendra, *Phys. Rev. D* **105**(6), 063533 (2022). DOI 10.1103/PhysRevD.105.063533
 47. H.V. Ragavendra, P. Saha, L. Sriramkumar, J. Silk, *Phys. Rev. D* **103**(8), 083510 (2021). DOI 10.1103/PhysRevD.103.083510
 48. S. Garcia-Saenz, L. Pinol, S. Renaux-Petel, D. Werth, *JCAP* **03**, 057 (2023). DOI 10.1088/1475-7516/2023/03/057
 49. K.T. Abe, R. Inui, Y. Tada, S. Yokoyama, *JCAP* **05**, 044 (2023). DOI 10.1088/1475-7516/2023/05/044
 50. R.g. Cai, S. Pi, M. Sasaki, *Phys. Rev. Lett.* **122**(20), 201101 (2019). DOI 10.1103/PhysRevLett.122.201101
 51. C. Unal, *Phys. Rev. D* **99**(4), 041301 (2019). DOI 10.1103/PhysRevD.99.041301
 52. V. Atal, G. Domènech, *JCAP* **06**, 001 (2021). DOI 10.1088/1475-7516/2021/06/001
 53. C. Yuan, Q.G. Huang, *Phys. Lett. B* **821**, 136606 (2021). DOI 10.1016/j.physletb.2021.136606
 54. F. Zhang, *Phys. Rev. D* **105**(6), 063539 (2022). DOI 10.1103/PhysRevD.105.063539
 55. J. Lin, S. Gao, Y. Gong, Y. Lu, Z. Wang, F. Zhang, *Phys. Rev. D* **107**(4), 043517 (2023). DOI 10.1103/PhysRevD.107.043517
 56. L.Y. Chen, H. Yu, P. Wu, *Phys. Rev. D* **106**(6), 063537 (2022). DOI 10.1103/PhysRevD.106.063537
 57. Z. Chang, Y.T. Kuang, D. Wu, J.Z. Zhou, Q.H. Zhu, *Phys. Rev. D* **109**(4), L041303 (2024). DOI 10.1103/PhysRevD.109.L041303
 58. R.G. Cai, S. Pi, S.J. Wang, X.Y. Yang, *JCAP* **10**, 059 (2019). DOI 10.1088/1475-7516/2019/10/059
 59. G. Perna, C. Testini, A. Ricciardone, S. Matarrese, *JCAP* **05**, 086 (2024). DOI 10.1088/1475-7516/2024/05/086
 60. X.X. Zeng, R.G. Cai, S.J. Wang, *JCAP* **10**, 045 (2024). DOI 10.1088/1475-7516/2024/10/045
 61. L. Valbusa Dall'Armi, A. Ricciardone, N. Bartolo, D. Bertacca, S. Matarrese, *Phys. Rev. D* **103**(2), 023522 (2021). DOI 10.1103/PhysRevD.103.023522
 62. E. Dimastrogiovanni, M. Fasiello, A. Malhotra, P.D. Meerburg, G. Orlando, *JCAP* **02**(02), 040 (2022). DOI 10.1088/1475-7516/2022/02/040
 63. P. Auclair, et al., *Living Rev. Rel.* **26**(1), 5 (2023). DOI 10.1007/s41114-023-00045-2
 64. C. Ūnal, E.D. Kovetz, S.P. Patil, *Phys. Rev. D* **103**(6), 063519 (2021). DOI 10.1103/PhysRevD.103.063519
 65. A. Malhotra, E. Dimastrogiovanni, G. Domènech, M. Fasiello, G. Tasinato, *Phys. Rev. D* **107**(10), 103502 (2023). DOI 10.1103/PhysRevD.107.103502
 66. L. Valbusa Dall'Armi, A. Mierna, S. Matarrese, A. Ricciardone, (2023). DOI 10.48550/arXiv.2307.11043
 67. C.R. Contaldi, *Phys. Lett. B* **771**, 9 (2017). DOI 10.1016/j.physletb.2017.05.020

-
68. R.K. Sachs, A.M. Wolfe, *Astrophys. J.* **147**, 73 (1967). DOI 10.1007/s10714-007-0448-9
 69. S. Kuwahara, L. Tsukada, (2024). DOI 10.48550/arXiv.2411.19761
 70. Z.C. Liang, Z.Y. Li, E.K. Li, J.d. Zhang, Y.M. Hu, *Phys. Rev. D* **111**(4), 043032 (2025). DOI 10.1103/PhysRevD.111.043032
 71. C. Tian, R. Ding, X.X. Kou, *JCAP* **08**, 037 (2025). DOI 10.1088/1475-7516/2025/08/037
 72. A. Ly, M. Marsman, J. Verhagen, R. Grasman, E.J. Wagenmakers. A tutorial on fisher information (2017). URL <https://arxiv.org/abs/1705.01064>
 73. F. Jenet, L.S. Finn, J. Lazio, A. Lommen, M. McLaughlin, I. Stairs, D. Stinebring, J. Verbiest, A. Archibald, Z. Arzoumanian, D. Backer, J. Cordes, P. Demorest, R. Ferdman, P. Freire, M. Gonzalez, V. Kaspi, V. Kondratiev, D. Lorimer, R. Lynch, D. Nice, S. Ransom, R. Shannon, X. Siemens. The north american nanohertz observatory for gravitational waves (2009). URL <https://arxiv.org/abs/0909.1058>
 74. J. Baker, et al., (2019). DOI 10.48550/arXiv.1907.06482
 75. T.L. Smith, T.L. Smith, R.R. Caldwell, R. Caldwell, *Phys. Rev. D* **100**(10), 104055 (2019). DOI 10.1103/PhysRevD.100.104055. [Erratum: *Phys.Rev.D* 105, 029902 (2022)]
 76. J. Crowder, N.J. Cornish, *Phys. Rev. D* **72**, 083005 (2005). DOI 10.1103/PhysRevD.72.083005
 77. T.L. Smith, R. Caldwell, *Phys. Rev. D* **95**(4), 044036 (2017). DOI 10.1103/PhysRevD.95.044036
 78. N. Seto, S. Kawamura, T. Nakamura, *Phys. Rev. Lett.* **87**, 221103 (2001). DOI 10.1103/PhysRevLett.87.221103
 79. S. Kawamura, et al., *PTEP* **2021**(5), 05A105 (2021). DOI 10.1093/ptep/ptab019
 80. S. Hild, S. Chelkowski, A. Freise, (2008). DOI 10.48550/arXiv.0810.0604
 81. D. Reitze, et al., *Bull. Am. Astron. Soc.* **51**(7), 035 (2019). DOI 10.48550/arXiv.1907.04833
 82. N. Pol, S.R. Taylor, J.D. Romano, *Astrophys. J.* **940**(2), 173 (2022). DOI 10.3847/1538-4357/ac9836
 83. M. Braglia, S. Kuroyanagi, *Phys. Rev. D* **104**(12), 123547 (2021). DOI 10.1103/PhysRevD.104.123547
 84. M. Tegmark, D.J. Eisenstein, W. Hu, A. de Oliveira-Costa, *Astrophys. J.* **530**, 133 (2000). DOI 10.1086/308348
 85. G. Cusin, I. Dvorkin, C. Pitrou, J.P. Uzan, *Phys. Rev. Lett.* **120**, 231101 (2018). DOI 10.1103/PhysRevLett.120.231101
 86. G. Cusin, C. Pitrou, J.P. Uzan, *Phys. Rev.* **D96**(10), 103019 (2017). DOI 10.1103/PhysRevD.96.103019
 87. G. Cusin, I. Dvorkin, C. Pitrou, J.P. Uzan, *Mon. Not. Roy. Astron. Soc.* **493**(1), L1 (2020). DOI 10.1093/mnrasl/slz182
 88. G. Cusin, I. Dvorkin, C. Pitrou, J.P. Uzan, *Phys. Rev. D* **100**(6), 063004 (2019). DOI 10.1103/PhysRevD.100.063004
 89. A.C. Jenkins, R. O’Shaughnessy, M. Sakellariadou, D. Wysocki, *Phys. Rev. Lett.* **122**(11), 111101 (2019). DOI 10.1103/PhysRevLett.122.111101
 90. A.C. Jenkins, M. Sakellariadou, T. Regimbau, E. Slezak, *Phys. Rev. D* **98**(6), 063501 (2018). DOI 10.1103/PhysRevD.98.063501
 91. A.C. Jenkins, J.D. Romano, M. Sakellariadou, *Phys. Rev. D* **100**(8), 083501 (2019). DOI 10.1103/PhysRevD.100.083501
 92. S. Wang, V. Vardanyan, K. Kohri, *Phys. Rev. D* **106**(12), 123511 (2022). DOI 10.1103/PhysRevD.106.123511
 93. S. Mukherjee, J. Silk, *Mon. Not. Roy. Astron. Soc.* **491**(4), 4690 (2020). DOI 10.1093/mnras/stz3226
 94. S.S. Bavera, G. Franciolini, G. Cusin, A. Riotto, M. Zevin, T. Fragos, *Astron. Astrophys.* **660**, A26 (2022). DOI 10.1051/0004-6361/202142208

95. N. Bellomo, D. Bertacca, A.C. Jenkins, S. Matarrese, A. Raccanelli, T. Regimbau, A. Ricciardone, M. Sakellariadou, *JCAP* **06**(06), 030 (2022). DOI 10.1088/1475-7516/2022/06/030
96. Y. Cui, S. Kumar, R. Sundrum, Y. Tsai, *JCAP* **10**, 064 (2023). DOI 10.1088/1475-7516/2023/10/064
97. Z.C. Zhao, S. Wang, *Sci. China Phys. Mech. Astron.* **67**(12), 120411 (2024). DOI 10.1007/s11433-024-2498-0